Large Seebeck Voltage of Co, Mn, Ni, Fe-Ceramics

Wilfried Wunderlich

Tokai University, Graduate School of Engineering, Department of Material Science,
259-1292 Hiratsuka-shi, Kitakaname 4-1-1, Japan
wi-wunder@rocketmail.com

Abstract

Thermoelectric materials based on Cobaltites are known for their large Seebeck coefficient. This paper reports about Seebeck voltage measurements under large temperature gradient of conventionally sintered Cobalt oxides alloyed with Mn, Ni or Fe. The results show a large positive Seebeck coefficient and short-circuit current and large negative Seebeck coefficient for Co50 Ni50 Fe10 oxides. The discussion focuses on the comparison with phase diagrams and indicates that a large Seebeck coefficient does not necessarily require the spinel structure.

Keywords

N- and P-type Thermoelectric Oxides; Seebeck Coefficient; Spinel; Microstructure

Introduction

Two kinds of famous thermoelectric oxides with large Seebeck coefficient and figure-of-merit are based on cobaltite. $NaCoO_{3-x}$ is known for the spin contribution to the thermoelectric power [Terasaki 1997] and with intercalation it turns into a superconductor [Takada 2003]. $CaCoO_3$ is known as stable thermoelectric for power generation [Funahashi 2000, Pinitsoontorn 2012] and its performance is explained by spin frustration on the Kagome lattice [Koshibae 2000].

The CoNiMn oxide system and its extensions to iron oxide has the advantage that no low melting eutectic point occurs and all components are stable up to 1500 ^{o}C, a necessary condition for power generation up to high temperatures. Also, the electric conductivity σ is larger compared to other ceramics. Besides the fact that thermoelectric materials require a large Seebeck coefficient S, and a small thermal conductivity κ, in order to achieve a large figure of merit $ZT = S^2 T\sigma / \kappa$. The system has been considered as a candidate for thermoelectric material [Plewa 2004, Yokoyama 2012] already, but it is better known for thermistor applications, for which materials with negative temperature coefficient (NTC) [Abe 1999, Yokoyama 2007, Park 2005] are required. In this system interesting findings have been reported [Yokoyama 2012]. The electrical conduction of the oxides is controlled by the small polaron hopping mechanism. The carrier concentration can be controlled independently from the mobility [Yokoyama 2012].

The formation of the Spinel region in this ternary CoMnNi oxide system has been sketched on a structural map [Abe 2008]. The $(Co,Mn)_3O_4$ spinel is stable over a wide temperature and composition range. The relationship between average cation radii and oxygen parameter has been examined for various spinels and inverse spinels [Yokoyama 2005]. The activation energies for the temperature dependence of the electric conductivity are correlated to the composition. In systems with the neighbouring Fe element the formation of similar spinel structures is observed [Rohrer 2004], such as the inverse Spinel structure in $Co_{3-x}Fe_xO_4$ [Rohrer 2004], $NiFe_2O_4$ [Bahlawane 2009] or $NiMn_2O_4$, [Rohrer 2004, Tsukimura 2003, Feteira 2009] also known as NTC ceramic with a report of detailed resistivity measurements. Another application of Co_2MnO_4 spinel has recently been reported, which is the discovery of its large catalytic oxidation behaviour [Bordeneuve 2009].

In Co-based rare earth ceramics we have reported [Wunderlich 2011] new thermoelectric phenomena related to measurements under high temperature gradient, while conventional $NaTaO_3$-Fe_2O_3 composite ceramics show completely linear Seebeck coefficient over a wide temperature range [Wunderlich 2010, Wunderlich 2009]. The research reported in this paper has three goals, the first one is to verify thermoelectric properties of the CoNiMn system, the second one is to

check in other systems and the third is to find the guiding principles for further search.

Experimental

Specimens were produced by conventional sintering. Firstly, well-defined weight ratios of fine powders of a black CoO-Co_3O_4 powder (Fine Chemicals Ltd.) were mixed with pure metals Mn, Ni or Fe, in a mortar for more than 10min. The specimens were pressed with 100 MPa as pellets 15 mm in diameter and 3mm height and sintered in air at 1273 K for 5 h in an air furnace with slow heating and cooling rates (100 K/h). The metal oxidation should provide some additional heat for alloy formation known as reaction sintering. The specimens were characterized by SEM (Hitachi 3200-N) at 20kV equipped with EDS (Noran) mapping. The properties were characterized by electric resistivity measurements (Sanwa PC510).

The thermoelectric measurements were performed by a self-manufactured device as reported previously. The specimen lied with one side on a copper block as a heat sink and with its other side on a micro-ceramic heater (Sakaguchi Ltd. MS1000), which was heated up to 1273 K within 3 min. Hence, the bottom part of the specimen experiences a large temperature difference of 650 K at maximum heating. The upper part is heated through the heat diffusivity of the specimen. From temperature distribution as measured by thermocouples the Seebeck voltages were measured by Sanwa PC510 voltmeters and recorded online by a personal computer. From the temperature dependence of Seebeck voltage U_{See} the Seebeck coefficient $S = \Delta U_{See} / \Delta T$ was calculated. This Seebeck coefficient measurement is performed under a large temperature gradient with maximum ΔT =650K, which is close to the condition in applications like thermo-generators using gas burners. During measurement the upper temperature gradually increases, while the lower temperature is kept constant. So we can measure a temperature dependence of the Seebeck coefficient $S(\Delta T)$, which, however, is slightly different from the $S(T)$ with ΔT << 10K usual measured by ZEM (Ulvac) as provided in literature. When the specimen has a linear Seebeck coefficient with temperature $S(T)$, the same Seebeck coefficient $S(\Delta T) = S(T)$ is measured, which was confirmed und will be published soon.

When the maximum temperature was reached and the Seebeck voltage was stabilized, the open ends of cold and hot specimen sides were closed by different resistors (1, 10, 100, 1k, 10k, 100k, 1MΩ) and the current measured. This closed circuit current is a measure for its performance [Wunderlich 2012]. In ideal case, when the specimen has small resistivity, a large Seebeck voltage will cause a large current, but some specimens behave differently due to the internal resistance of the specimen, namely charge carrier concentration and mobility.

Results and Discussion

The sintered specimens show a dense microstructure (fig.1) with a grain size of about 1 μm. There is not much difference between the microstructure of the three alloys (a) Co_{48} Ni_{52} (b) Co_{42} Ni_{20} Fe_{40} (c) Co_{54} Mn_{15} Ni_{15} Fe_{15} oxide ceramics. An exception is only case (c), which is the alloy with the largest amount of additions.

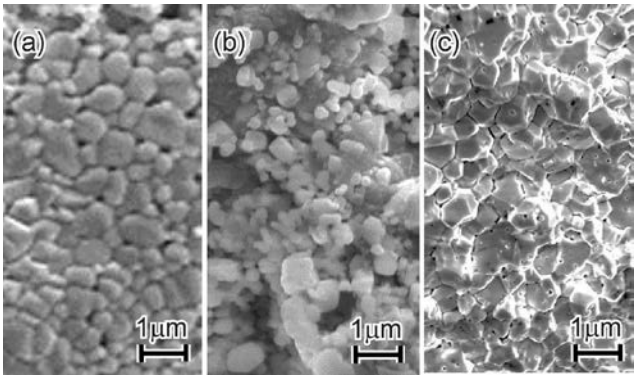

FIGURE 1 SEM MICROGRAPH OF (A) CO48 NI52 (B) CO42 NI20 FE40 (C) CO54 MN15 NI15 FE15 OXIDE CERAMICS

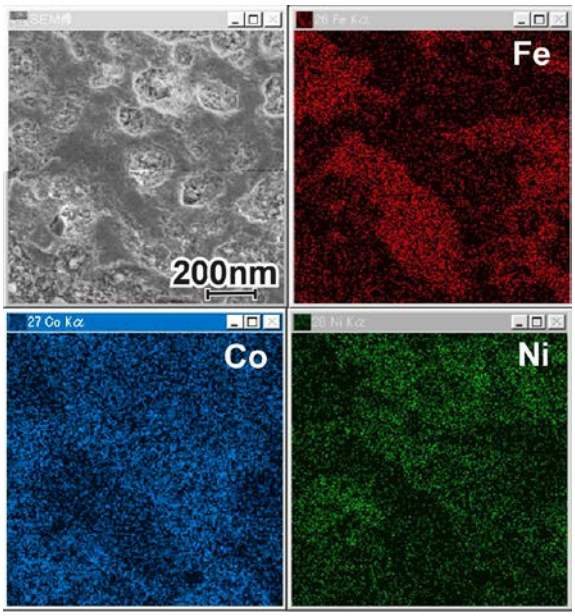

FIGURE 2 SEM MICROGRAPH AND EDS MAPPING OF CO41 NI20 FE40 OXIDE CERAMICS

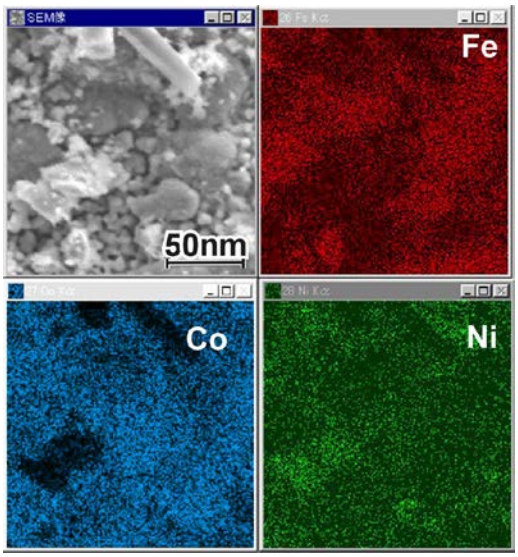

FIGURE 3 SEM MICROGRAPH AND EDX MAPPING OF CO51 NI16 FE33 OXIDE CERAMICS

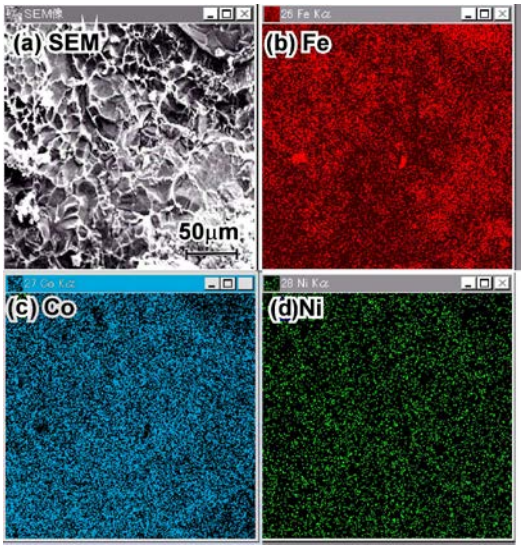

FIGURE 4 SEM MICROGRAPH AND EDS MAPPING OF CO80 NI11 FE10 OXIDE CERAMICS

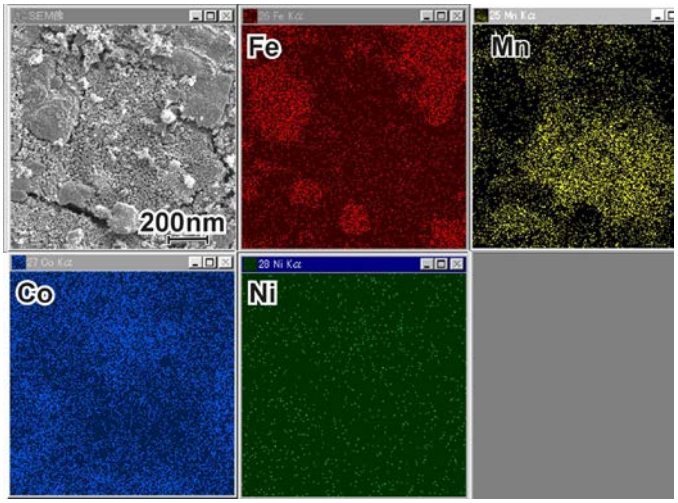

FIGURE 5 SEM MICROGRAPH AND EDS MAPPING OF CO41 NI14 FE30 MN15 OXIDE CERAMICS

On large magnification the specimens after sintering still show small pores inside the grains, obviously stoichiometric vacancies due to large deviation from the starting composition. Apparently, the sintering time was not long enough to compensate the oxygen content according to the change in valence after diffusion of the different metal species.

In the following the chemical mapping by EDS is shown in the same color code for each of the elements, Co, Fe, Ni and Mn. The maps confirmed that the ceramic alloys are already almost homogenous, at least for Co. Fig. 2 shows that Fe-rich parts appear, while Ni-rich parts are separated. The EDS mapping shown in Fig. 3 confirms this fact also for the specimen with a little larger Co concentration, Co51 Ni16 Fe33. When Co concentration further increases (Co80 Ni11 Fe10, fig. 4), the element distribution becomes almost homogeneous. Fig.5 shows the Co41 Ni14 Fe30 Mn15, which contained all tested elements. Mn and Fe still show inhomogeneous concentrations.

The conclusion from the SEM characterization part is that the more elements the composite contains, the longer it takes to homogenize the specimen. Co has a fast diffusion coefficient, Ni also to some extent, while Fe and Mn are slow.

The Seebeck voltage as function of the temperature gradient is shown in figs. 6 - 10 (a), where the red line marks the heating, the blue line the cooling and the hatched line the Seebeck coefficient as average slope. The $Co_{50}Ni_{10}Fe_{40}O_x$ specimen shows a negative Seebeck coefficient of S = -0.15 mV/K (fig. 6a), the $Co_{54}Ni_{12}Fe_{38}O_x$ specimen shows a negative Seebeck coefficient of S = -0.2 mV/K (fig. 7 a), the $Co_{48}Ni_{52}O_x$ specimens shows a negative Seebeck coefficient of S = -0.35 mV/K (fig. 8a) and S = -0.45 mV/K (fig. 9a), while the Co_{54} Mn_{15} Fe_{30} O_x shows a positive one of S = 0.08 mV/K (fig.10 a). When heating the specimens, the maximum Seebeck voltage is reached at a temperature difference of 550K to 600K as indicated by the orange curve in figs. 6 (a) to 10 (a). During cooling the Seebeck voltage decreases faster than expected from the heating, as indicated by the blue curve in fig. 6 (a) to 7 (a). The shape of the non-linearity is considered as a kind of fingerprint of the activated carrier concentration and the electron-phonon coupling. When the Ni content (fig. 8 (a) and 9 (a)) increases, the Seebeck voltage decreases almost linearly. Hence, we can conclude, with increasing Ni-content (fig. 6 (a) to 10 (a)) the strong non-linearity in the Seebeck voltage-versus-temperature disappears.

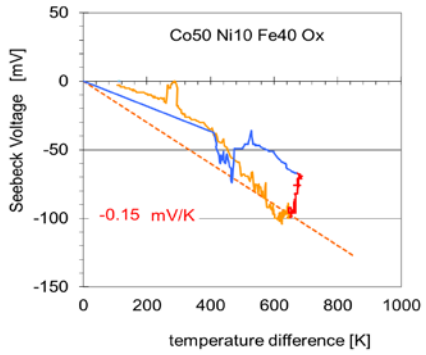

(a)

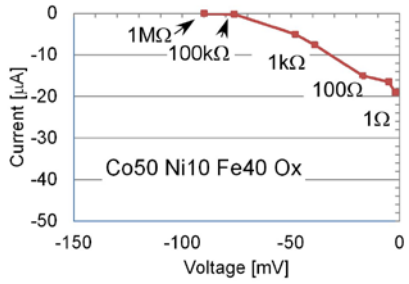

(b)

FIGURE 6 SEEBECK VOLTAGE MEASUREMENTS FOR CO_{50} NI_{102} FE_{40} OXIDE (A) TEMPERATURE DEPENDENCE, (B) SHORT CIRCUIT CURRENT

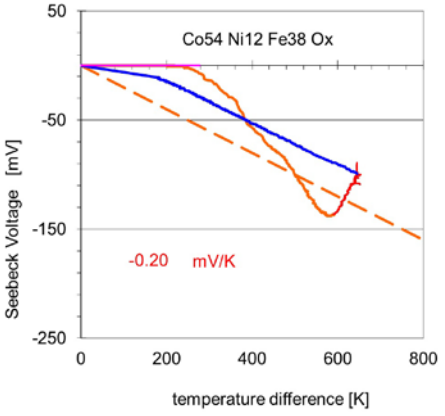

(a)

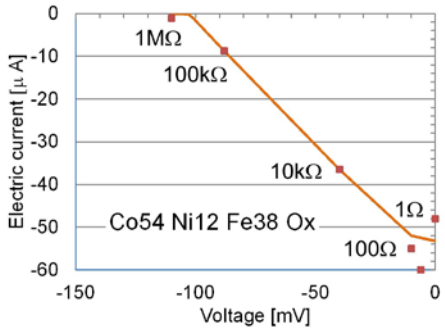

(b)

FIGURE 7 SEEBECK VOLTAGE MEASUREMENTS FOR CO_{54} NI_{12} FE_{38} OXIDE (A) TEMPERATURE DEPENDENCE, (B) SHORT CIRCUIT CURRENT

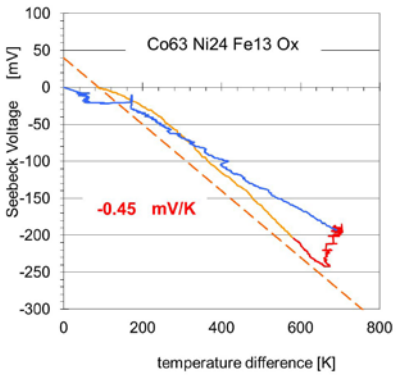

(a)

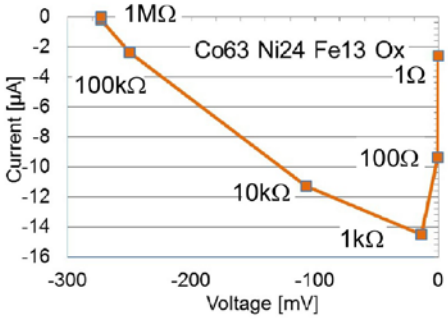

(b)

FIGURE 8 SEEBECK VOLTAGE MEASUREMENTS FOR CO_{63} NI_{24} FE_{13} OXIDE (A) TEMPERATURE DEPENDENCE, (B) SHORT CIRCUIT CURRENT

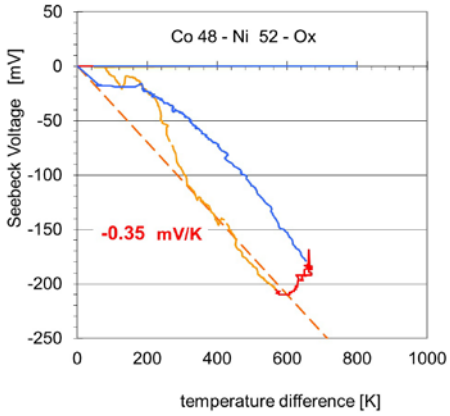

(a)

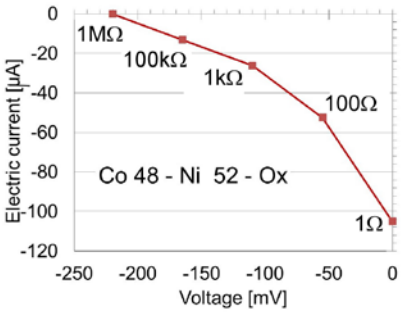

(b)

FIGURE 9 SEEBECK VOLTAGE MEASUREMENTS FOR CO_{48} NI_{52} OXIDE (A) TEMPERATURE DEPENDENCE, (B) SHORT CIRCUIT CURRENT

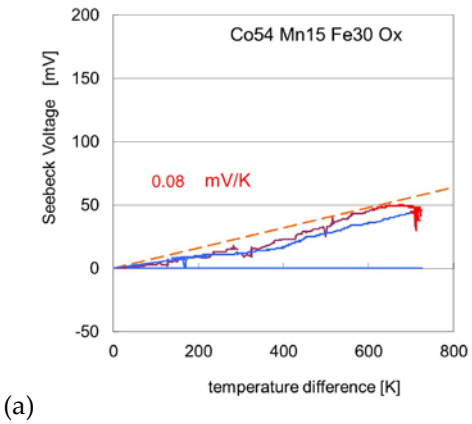

(a)

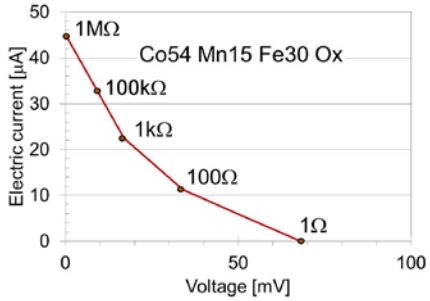

(b)

FIGURE 10 SEEBECK VOLTAGE MEASUREMENTS FOR CO54 MN15 FE30 OXIDE (A) TEMPERATURE DEPENDENCE, (B) SHORT CIRCUIT CURRENT

When the specimens are short-circuited with a load resistance, we can measure the Seebeck voltage-current, *U-I*-characteristic as shown in fig. 6 (b), where the values of the load resistance are marked.

The maximum current is -20 µA (fig. 6b), -50 µA (fig. 7 b), -14 µA (fig. 8b) and -100 µA (fig. 9b), and +45 µA (fig. 10 b). While the specimen shown in fig. 7 (b) has almost a linear *I-U*-characteristics, and the specimen in fig. 8 (b) shows a concave curve, the others show smaller currents than linearity, which means less power. These two specimens (fig 9a and 10a) are among the best of all specimens, large n- or p-type Seebeck voltage and fairly large closed circuit current.

In this survey about forty specimens with different compositions have been produced. The maximum Seebeck voltage at the temperature difference of ΔT = 650K are summarized in a map shown in fig. 10. The center shows the Co-Ni-Mn oxides, while the three attached triangles show the extension versus Fe oxides. The specimens with positive Seebeck coefficient are marked in red, those with negative are marked in blue, no Seebeck effect is marked in green and unobserved areas in white. The largest positive Seebeck coefficient of S = +0.29 mV/K is observed for Co_{25} Mn_{75} Ox, the largest n-type S = - 0.35 mV/K for Co_{48} Ni_{52} O_x. Fig. 11 shows the closed circuit current at ΔT = 650K. The largest p-type with I_{max} = +100 µA is observed for Co_{66} Mn_{33} Ox, which has however only S = 0.04mV/K. In the case of n-type behaviour, the largest specimen with largest current corresponds closely to that of largest Seebeck coefficient (Co_{37} Ni_{38} Fe_{24} versus Co_{48} Ni_{52}).

In order to discuss this behaviour we shown the structural map of the $(Co,Mn)_3O_4$ spinel in fig 12 [Abe 1999]. The yet unknown Fe system is attached and their inverse spinel phases Fe_2NiO_4 and Co_2FeO_4 and $(Mn,Co)_2FeO_4$ are marked.

The comparison with the structure map (fig. 12) to the properties map in fig 10 and 11 allows us to conclude which crystal structure is best for good thermoelectric performance. The material with largest positive Seebeck coefficient has obviously the Mn_2CoO_4 spinel structure. In the case of negative Seebeck coefficient it is not so obvious. It lies surprisingly in the $(Co,Ni)_3O_4$ region with NaCl structure or in the two phase region towards $NiFe_2O_4$. This fact leads to the conclusion that rather than crystal structure the interatomic bonding and the mixed valence are more important factors for good thermoelectric performance. Further investigations of the white areas are necessary to confirm this statement.

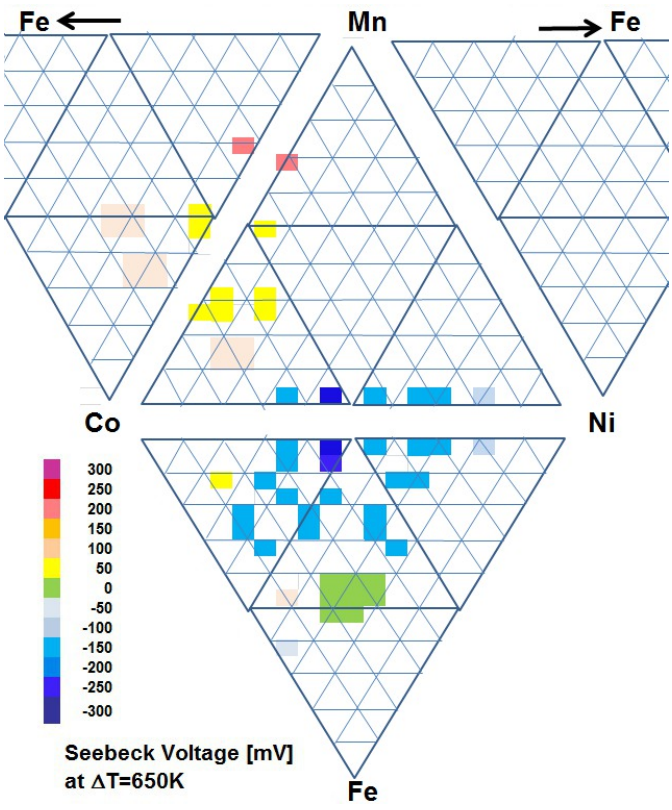

FIGURE 10 MAP OF THE QUATERNARY CO-NI-MN-FE OXIDE CERAMICS WITH MEASURED SEEBECK VOLTAGE AT ΔT =650K

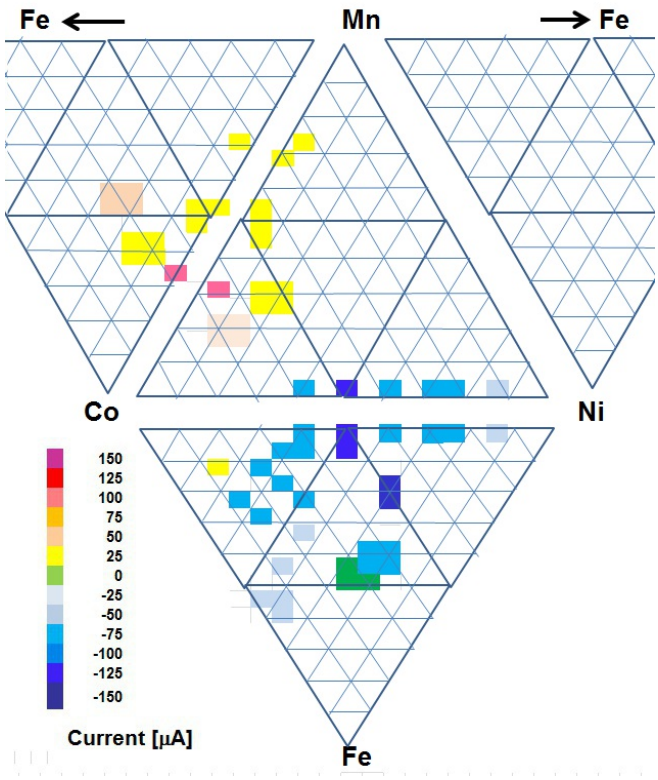

FIGURE 11 MAP OF THE QUATERNARY CO-NI-MN-FE OXIDE CERAMICS WITH MEASURED SHORT CIRCUIT CURRENT AT ΔT=650K

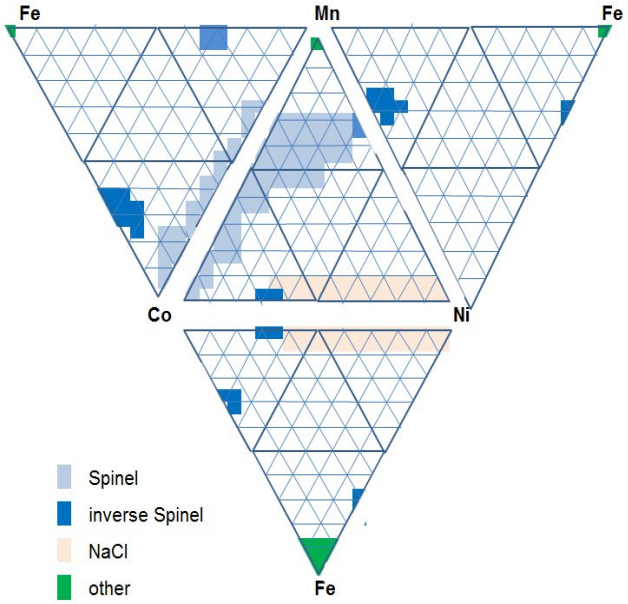

FIGURE 12 MAP OF THE QUATERNARY CO-NI-MN-FE OXIDE CERAMICS SHOWING THEIR CRYSTAL STRUCTURE

Conclusions

1. The Seebeck coefficient and short-circuit current of the Co-Mn-Ni- and the neighboring Fe- oxide ceramic system have been measured and compared to the crystal structure map.
2. The best p-type behavior is observed for $CoMn_2O_4$ or Co_2MnO_4, while the best n-type behavior is observed for $(Co,Ni)_3O_4$. A nonlinear Seebeck voltage is observed in specimens with larger Fe-content.
3. Co diffuses fast, while Mn diffusion is the slowest.
4. Rather than the crystal structure the interatomic bonding and the mixed valence seem to determine the Seebeck coefficient in these ceramic systems.

REFERENCES

Abe, Y., Meguro, T., Yokokawa, T., Komeya, K., *Formation region of monophase with cubic spinel-type oxides in Mn Co Ni ternary system*, J. Mat. Sci 34 (1999) 4639

Bahlawane, N. et al., *Tailoring the properties and the reactivity of the spinel cobalt oxide,* Phys. Chem. Chem. Phys., 11 (2009) 9224–9232

Bordeneuve, H., Guillement-Fritsch, S., Rousset, A., Schuurman, S., Poulain, V., *Structure and electrical properties of single-phase cobalt manganese oxide spinels Mn3−xCoxO4 sintered classically and by spark plasma sintering (SPS),* J. Solid State Chemistry 182 (2009) 396–401

Feteira, A., *Negative Temperature Coefficient Resistance (NTCR) Ceramic Thermistors: An Industrial Perspective*, J. Am. Ceram. Soc., 92 [5] 967–983 (2009)

Funahashi, R., Matsubara, I., Ikuta, H., Takeuchi, T., Mizutani, U., and Sodeoka, S., *An Oxide Single Crystal with High Thermoelectric Performance in Air*, Jpn. J. Appl. Phys. 39 (2000) L1127

Hastings, J.M., Corliss, L.M., *Neutron .Diffraction Studies of Zinc ferrite and:Nickel Ferrite*, Rev. Mod. Phys. 25 (1953) 114

Koshibae, W., Tsutsui, K., and Maekawa, S., *Thermopower in cobalt oxides,* Phys. Rev. B 62 11 6869 (2000)

Park, K., *Fabrication and Electrical Properties of Mn–Ni–Co–Cu–Si Oxides Negative Temperature Coefficient Thermistors,* J. Am. Ceram. Soc., 88 [4] 862–866 (2005)

Pinitsoontorn, S., Lerssongkram, N., Keawprak, N., Amornkitbamrung, V., *Thermoelectric properties of transition metals-doped* $Ca_3Co_{3.8}M_{0.2}O_{9+d}$ *(M = Co, Cr, Fe, Ni, Cu and Zn),* J Mater Sci: Mater Electron 23 [5] (2012)

1050–1056.

Plewa, J., Shpotiu, P.M.. Sopicka-Lizef, K., Kozlowskal, G., Plescha, N., Brunets, E., Brunets, I., and Altenburg, H. (2004) *Ceramic powder for thermoelectric, thermoresistive and superconducting materials* In: Proc. 8th Eur. Workshop on Thermoelectrics, Cracow, Poland (2004) pp. 1-6.

Rohrer, G.S., *Structure and Bonding in Crystalline Materials,* Cambridge Univ. Press (2004)

Savic, S. M., Stojanovic, A G. M., Nikolic, A M. V., Aleksic, A O. S., Lukovic-Golic, A D. T., Nikolic, A P. M., *Electrical and transport properties of nickel manganite obtained by Hall effect measurements*, J Mater Sci Mater Electron 20 (2009) 242–247

Takada, K., Sakural, H., Takayama-Muromachi, E., Izumi, F., Dilanian, R. A., and Sasaki, T., *Superconductivity in two-dimensional CoO2 layers*, Nature (London) **422**, 53 (2003).

Terasaki, I., Sasago, Y., and Uchinokura, K., *Large thermoelectric power in $NaCo_2O_4$ single crystals*, Phys. Rev. B **56**, R12685 (1997)

Tsukimura, K., Sasaki, S., Kimizuka, N., *Cation Distribution in Nickel Ferrites,* Jpn. J. Appl. Phys 36 (1997) 3609-12

Wunderlich 2009, W., *$NaTaO_3$ composite ceramics - a new thermoelectric material for energy generation,* J Nucl. Mat. 389 [1] (2009) 57-61,

Wunderlich 2010, W., Soga, S., *Microstructure and Seebeck voltage of Mn,Cr,Fe,Ti- added $NaTaO_3$ composite ceramics,* Journal of Ceramic Processing Research. Vol. 11, No. 2, pp. 233-236 (2010)

Wunderlich 2011a, W., Fujiwara, H., *The Difference between thermo- and pyroelectric Co- based RE-(= Nd, Y, Gd, Ce)-oxide composites measured by high-temperature gradient,* J. Electronic materials 40 [2] (2011) 127-133

Wunderlich 2011b, W., Motoyama, Y., Sugisawa, Y. and Matsumura, Y., *Large Seebeck Closed-Circuit Currents in Quaternary (Ti,Zr)NiSn Heusler-Alloys,* J. Electronic Materials, 40 [5] 583-588 (2011)

Wunderlich 2012, W., Shinohara, Y. and Matsumura, Y., *Magnetron Sputtering of (Ti,Zr)NiSn Thin Films on Si (111) wafers for thermoelectric applications,* J. Phys.: Conf. Ser. 379 (2012) 012005

Yokoyama, T., Meguro, A T., *Relationship between Average Cation Radii and Oxygen Parameter for Various Oxides with Spinel-Type Structure*, Jpn. J. Appl. Phys. 44(2005)6201

Yokoyama, T., Meguro, A T., Shimada, A Y., Tatami, A J., Komeya, A K., Abe, A Y., *Preparation and electrical properties of sintered oxides composed of Mn1.5Co(0.25+X)Ni(1.25-X)O4 (05X50:75) with a cubic spinel structure,* J Mater Sci 42 (2007) 5860–5866 DOI 10.1007/s10853-006-1141-1

Prof.Dr. Wilfried Wunderlich, educated and graduated in solid-state physics at Technical University Braunschweig. Germany, 1987 PhD degree obtained at Max-Planck Insitute for metal research, Stuttgart, Germany. Since 2001 guest professor at Nagoya Institute of Technology, Japan. Since 2006 teaching as associate professor and since 2012 as full professor at Tokai University, Faculty of Engineering, Department of Material Science, Hiratsuka, Japan.

He has long year experience in research on electrical properties of semiconductors, ceramics and metals. Research interests are finding principles for knowledge discovery and development of new alloys.

Prof. Dr. Wilfried Wunderlich, is a member of Ceramic society Japan (CSJ), German Physical Society (DPG), German Society of Materials (DGM), Japan Physics Society (JPS) and others. Invited talks at many international conferences. Referee for several scientific magazines including Phys.Rev. Scientific awards received in 1988 (Japan) and 1992 (Germany), awarded by prestigious JSPS fellowship in 1999 (Japan) and by the prestigious JST-CREST fellowship in 2004 (Japan).